Volcanic deformation models for Deception Island (South Shetland Islands, Antarctica)

A. Fernández-Ros, M. Berrocoso and M. E. Ramírez

Laboratorio de Astronomía, Geodesia y Cartografía. Departamento de Matemáticas. Facultad de Ciencias. Campus de Puerto Real. Universidad de Cádiz. 11510 Puerto Real (Cádiz-Andalucía). España (alberto.fernandez@uca.es)

Summary GPS observations from a Deception Island Volcano geodetic network (South Shetland Islands, Antarctica) during 1991/1992 to 2002/2003 campaigns have characterized the deformation of the island resulting from its volcanic activity. From January 1992 to December 1999, radial extension together with an uplift episode was detected. During this period two important episodes of seismic activity took place, in particular, during the campaigns 1991/92 and 1998/99. From 2000 until 2003, no large displacements were detected, although the stations seem to converge in a radially compressive manner together with a subsidence, reflecting a change in the geodynamics of the island. Two clear alignments are observed on the contour maps that characterize the deformation, one in the NW-SE direction until 2000 and another on in the NE-SW direction from 2000 to 2003, coinciding with the principal directions of the tectonic features of the region, the Hero Fracture Zone and the Bransfield Rift.

Citation: Fernández-Ros, A., M. Berrocoso and M. E. Ramírez (2007), Volcanic deformation models for Deception Island (Shout Shetland Islands, Antarctica), in Antarctica: A Keystone in Changing World – Online Proceedings of the 10th ISAES X, edited by A. K. Cooper and C. R. Raymond et al., USGS Open-File Report 2007-1047, Extended Abstract 094, 5 p.

Introduction

Deception Island is located in a very complex tectonic zone where several tectonic plates converge: The South American Plate, the Antarctic Plate and three minor plates, Scotia micro-plate, Phoenix micro-plate and South Shetland micro-plate (Baraldo, 1999). The former Phoenix microplate is now part of the Antarctic plate. It is delineated by the former spreading center (Drake Ridge) to the northwest, the Hero Fracture Zone to the southwest, the South Shetland subduction system to the southeast and the Shackleton Fracture Zone to the northeast. The microplate was formerly being subducted under the South Shetland Islands and Bransfield Strait, but several studies reveal that the subduction process is no longer active.

The active volcanism in this area is mainly located in the extensional core of Bransfield rift and is characterized by the presence of several emerged volcanoes like Deception, Penguin and Bridgeman Islands. In addition there are also numerous submarine volcanic centres which show different evolution stages, from the volcanic cone to its collapse, generated by the existing divergent tectonics (Canals, et al., 1997). These volcanic centres are 15 km base diameter and about 450 m high. In addition, there are around 34 small centres with a mean diameter of 2.5 km. These centres are aligned following the main direction of the basin.

The continuous volcanic activity in this area is manifested by historical eruptions at Deception and Penguin islands, together with the Bransfield central basin rifting and the magmatic processes in the rift during the last two million years. This fact suggests that the volcanic activity in the Bransfield basin is in continuous development (González-Ferrán, 1991).

REGID geodetic network

The geodetic network for Deception Island (REGID) was established from observations of GPS System satellites in order to set up the basic reference frame not only for the geodetic studies but also for other research. In this way, the network is the fundamental reference for the Spanish cartography in Antarctica, for geophysical and oceanographic observations and for hydrographical sounding carried out throughout the Spanish campaigns in the Antarctica. On the other hand, the GPS System accuracy, especially for horizontal positioning, makes the REGID network very useful for understanding geodynamic activity of the island.

Stations of the network

The establishment of the geodetic network began during the 1989-90 Antarctic campaign. The aim of the studies and the place where they were going to be carried out led to the construction of high stability benchmarks, with no visual impact. They were built with concrete, well-rooted in the permafrost with steel bars and at a low height above the ground. A standard screw was fixed in one of the corners of the post

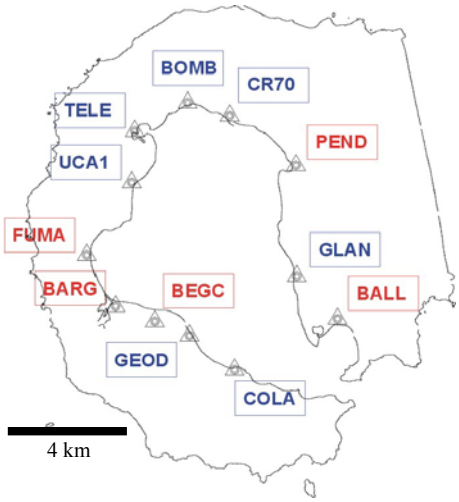

Figure 1. REGID geodetic network distribution.

for the use of geodetic instrumentation. Furthermore, some of the stations were built using existing structures of the buildings destroyed by the volcanic activity which happened between 1967 and 1970 (Berrocoso, 1997).

In the 1990-91 campaign, the geodetic network consisted of five stations, four of them in Deception Island (BARG, FUMA, PEND, BALL) and another one at the Spanish Base Juan Carlos I (BEJC) in Livingston Island. Their placements were chosen according to several factors, including accessibility, stability of the building, proximity of fumarolic areas, density of located epicenters, last eruptions.

During the 1995-96 campaign a new station was built near the Spanish Antarctic Base Gabriel de Castilla. This station (BEGC) was set as the new main point of the network. It has electric supply and it was built in the same way as the others (Berrocoso, 1997).

During the 2001-02 campaign seven more stations were built in the northern and southern part of Deception Island, in order to cover its entire inner ring and to make the REGID network coverage more consistent. The distribution of the stations is given in Figure 1. The construction of these new stations was carried out according to the same geodetic directions as the earlier ones: clear GPS horizon, low multipath effect. The area where they were built was chosen taking into account the volcanic nature of the island, but without considering any prior volcanic activity (Vila, 1992; García et al., 1997; Ibáñez et al., 2000).

GPS data collection

Stations of the initial network have been observed from 1991-92during the Spanish Antarctic campaigns. BEGC station was included in the 1995-96 campaign, when it was observed for the first time. After the construction of seven new stations in the 2001-02 campaign, COLA, GEODEC, UCA1, TELE BOMB, CR70 and GLAN, the whole network has been observed during the austral summers periods since the 2001-02 campaign to present. The triangle determined by BEGC, FUMA and PEND is continuously observed during the whole surveying from 2002-03 campaign. Antennae height corrections and phase centre offsets were applied to the data. The sampling rate was set to 15 s. and the elevation mask was 10º.

Data processing and adjustment of the network

Data from GPS surveying in Deception Island were processed using the Bernese v4.2 software (Beutler et al., 2001) using precise ephemerides. Data from the IGS station OHIG was used to the adjustment of the network. It is situated at the Chilean Base O'Higgins in the Antarctic Peninsula, 150 km. away from Deception Island.

Every campaign was processed independently, fixing the coordinates of one of the stations of the network. BARG was the fixed station until 2001, and then it was changed to BEGC station. In the 1991-92 campaign, the coordinates for the fixed station BARG were obtained from the international campaign SCAR92. The precise absolute coordinates for the station were referred to the ITRF91, epoch 92.2. To get these coordinates for the next campaigns, in 1995-96 and 2001-02, the coordinates of OHIG corresponding to ITRF96, epoch 96.1 and to ITRF97, epoch 99.9, were fixed.

REGID WGS84 COORDINATES						
STATION	**Φ (S)**	**λ (W)**	**h (m)**	**σ_φ(m)**	**σ_λ (m)**	**σ_h(m)**
OHI2	63 19 15.8930	57 54 4.7999	32.469	FIXED	FIXED	FIXED
BEGC	62 58 43.6576	60 40 27.5304	82.070	0.001	0.001	0.002
BARG	62 58 30.2679	60 41 53.3601	22.283	0.001	0.001	0.006
BALL	62 58 38.5553	60 33 52.5089	25.968	0.003	0.001	0.006
FUMA	62 57 41.0170	60 42 59.3471	22.911	0.001	0.001	0.006
BEJC	62 39 46.7782	60 23 19.9915	31.241	0.002	0.001	0.009
PEND	62 56 9.8456	60 35 34.3437	28.841	0.001	0.001	0.003
COLA	62 59 27.9180	60 37 31.8014	48.050	0.003	0.001	0.009
GLAN	62 57 58.3621	60 35 23.8528	27.541	0.003	0.003	0.012
GEOD	62 58 56.4127	60 39 11.7290	42.182	0.003	0.001	0.009
UCA1	62 56 28.4103	60 41 28.0891	28.667	0.003	0.001	0.009
CR70	62 55 23.6706	60 38 1.0013	23.600	0.003	0.003	0.015
TELE	62 55 37.9905	60 41 25.5485	23.791	0.003	0.003	0.012
BOMB	62 55 8.4201	60 39 33.8481	23.785	0.003	0.003	0.015

Table 1. REGID geodetic network stations WGS84 coordinates (based on ITRF2000.0).

Due to the proximity of the BEGC station to the Spanish Base Gabriel de Castilla, the receiver is easily maintained and it is possible to collect data continuously during the campaign. That is why this station was considered as the main one in the network REGID from the 2001-02 campaign. Its coordinates were obtained by fixing the ones of OHIG corresponding to the ITRF2000, epoch 2000.0.

Once the coordinates of the fixed station were set, the coordinates for the rest of the stations in the network were obtained by means of radial baselines from the fixed site to the rest of the stations. Simultaneous observations were used for the processing of the data. In the 1991-92 campaign, the radial processed baselines were BARG- FUMA, BARG-PEND and BARG- BALL. The ambiguities were calculated by the SIGMA strategy of the BERNESE software, since the observations were made by single-frequency receivers. Finally, the results were reference to the ITRF91; in 1995-96, observations of both L1 and L2 frequencies were available, so the ambiguities resolution was solved applying the QIF strategy. The final solution was referenced to the ITRF96; in the 1999-00, the baselines were processed altogether since it was the first time that every station was observed simultaneously. The ambiguities were also resolved with the QIF strategy and the final solution was referenced to the ITRF97; from 2001-02 campaign, solutions for every week were combined with the ADDNEQ program of the BERNESE software. QIF strategy was also used and the final solution was referenced to the ITRF2000. To estimate the tropospheric delays we use the default meteorological data, since the only available data were the medium temperature and pressure and their inclusion could produce more errors than the models provided by the software. The final results are shown in Table 1. They are referenced to the ITR2000, epoch 2000.0.

Volcanic deformation models determination

Deformation models representing Deception Island volcanic activity were obtained from the GPS observations of the stations in the REGID geodetic network. GPS observations have been episodically made from 1991-92 campaign to present. Taking into account that GPS system provides accuracy twice better in horizontal positioning than in the elevation component, we distinguish between the horizontal and the vertical models, although it is essential to use both results together for a proper interpretation. (Donellan, A., 1993; El-Fiky et al. 1999; Calais et al., 2000; Mantovani et al., 2001; Murray and Wooller, 2002).

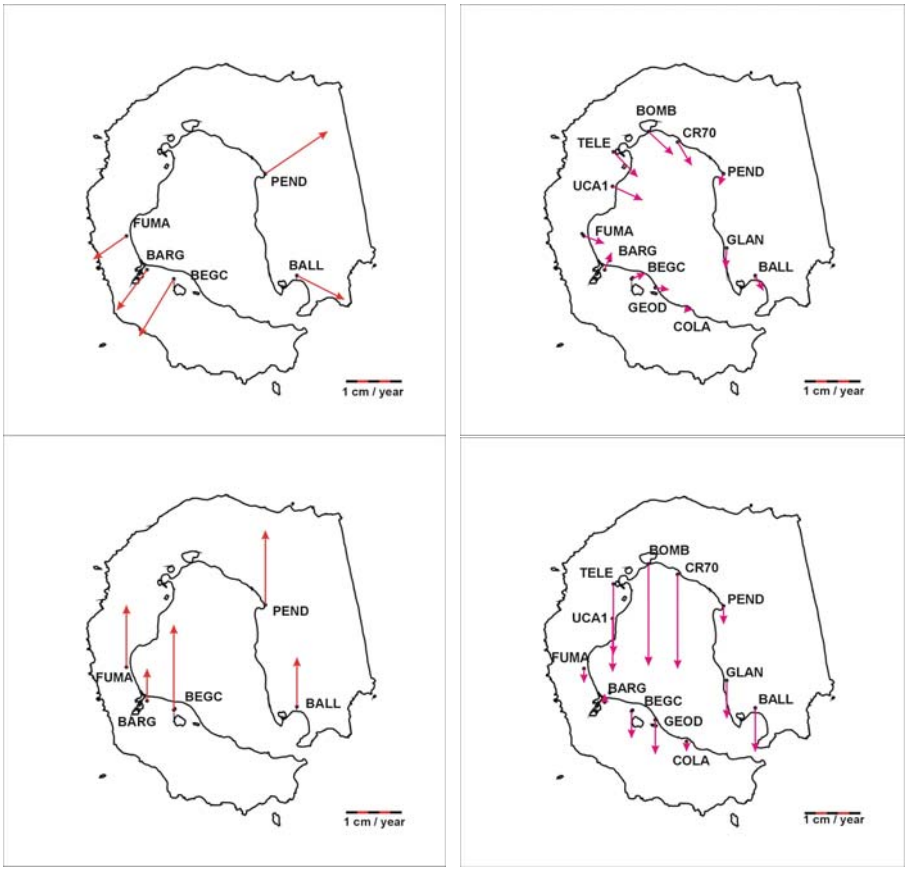

Figure 2. From left to right, up to bottom: horizontal and vertical deformation models for 1996.2/1999.9, and 2002.2/2003.2 epochs (cms/year), respectively.

To obtain the deformation models a topocentric system was established with origin at BARG. In order to obtain the absolute deformation of the island, BEJC station on Livingston Island was considered. Displacement models were calculated comparing absolute topocentric coordinates between two consecutives campaigns (Figure 2); the velocity fields and its gradient were determined by a finite elements interpolation; horizontal deformation tensors were calculated to obtain the deformation parameters, that is, the extension-compression area, determining the components in NS and EW directions (Dermanis, 1985; Eren, 1984; Vaníček et al., 1986). Finally, the geodetic maximum deformation is obtained (Grafarend and Voosoghi, 2003). Figure 3 shows the mathematical horizontal deformation models obtained from the displacement models by dilatation (Bibby, 1982; Ward, 1998; Drew and Snay, 1989; Dzurisin, 2006).

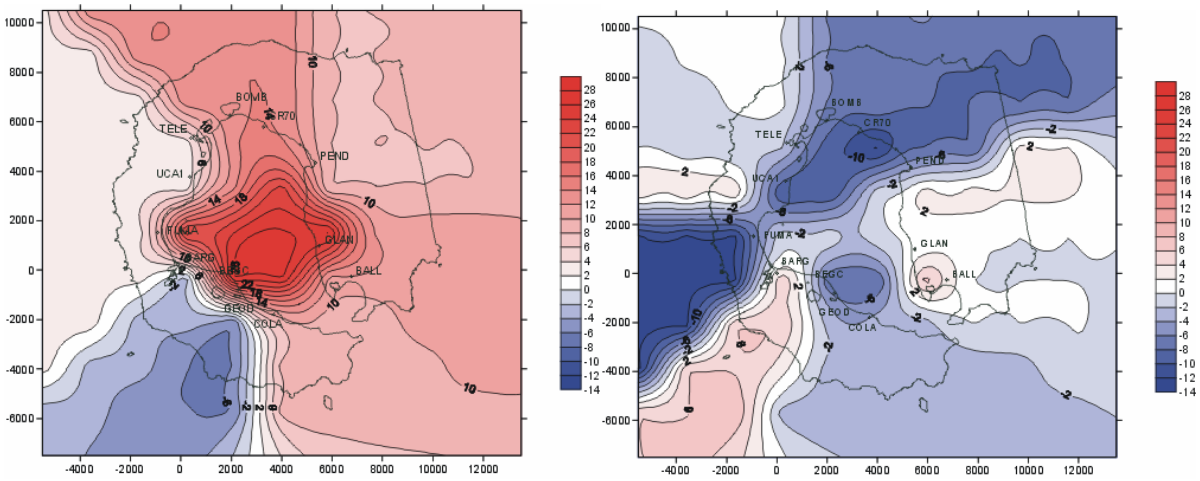

Figure 3. Superficial dilatation (ppm/year) from 1996.2/1999.9 and 2002.2/2003.2 epochs.

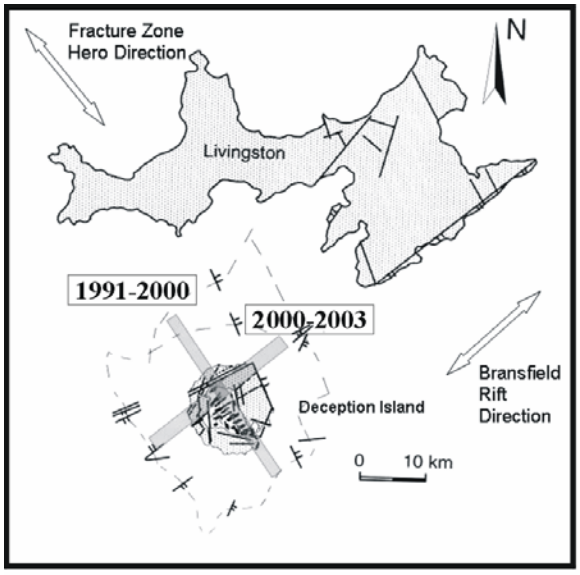

Figure 4. Principal directions of deformation process in Deception Island.

The analysis realized from 1991/1992 to 2002/2003 campaigns shows a radial extensional process from 1995/ 1996 to 1999/2000 campaign. Afterwards, the process became compressive. An uplift episode from 1995/1996 to 2001/2002 campaigns was detected, preceded and followed by a subsidence process. The extensional process follows a NW-SE direction (Fracture Hero Zone direction), while the compressive process follows the Bransfield Rift extensional direction (Fernández-Ros, 2006).

Acknowledgments. The realization of this work has been possible thanks to the financial support to the following projects: ANT1999-1430-e/HESP, DECVOL, REN 2000-0551-C03-01 GEODEC, REN2000-2690-E ,Acquisition of a Scientific Software for GPS data processing, and CGL2004-21547-E/ANT, VOLTEDEC, all of them funded by the Spanish Ministry of Science and Technology through the National Program of Antarctic Research of Natural Resources.

References

Baraldo, A. (1999), Evolución geológica de la Isla Decepción, Islas Shetland del Sur, Antártida. Ph. Tesis, Universidad de Buenos Aires. 213 pp.

Berrocoso, M. (1997), Modelos y formalismos para tratamiento de observaciones GPS. Aplicación a establecimiento de la Red Geodésica y Geodinámica Antártica. Boletín ROA núm 1/97, San Fernando (Cádiz).

Beutler, G., Bock, H., Brockmann, E. & Bernese Working Group (2001), BERNESE software Version 4.2. V. Hungentobler, S. Schaer, and P. Fridez, Astronomical Institute, University of Berne.

Bibby, HM. (1982), Unbiased estimated of strain from triangulation data using the method of simultaneous reduction. Tectonophysics. 82., 161-174.

Canals M, Gràcia E y Grupo GEBRA (1997), Evidence of initial seafloor spreading in the Central Bransfield Basin, Western Antarctica. Bol R Soc Esp Hist Nat (Sec Geolog) 93(1-4): 53-61.

Calais, E., Galisson, L., Stéphan. J.F., Delteil, J., Decerchère, J., Larrouque, C., Mercier De Lépinay, B., Popoff, M. And Sosson, M. (2000), Crustal strain in the Southern Alps, France, 1948-1998. Tectonophysics. 319, 1-17.

Dermanis, A. (1985), The Role of Frame Definitions in the Geodetic Determination of Crustal Deformation Parameters. Bulletin Geodesique, 59 (3), 247-274.

Donnellan, A. (1993), Geodetic measurement of deformation in the Ventura basin region, southern California. Journal of Geophysical Research, vol. 98, noB12, pp. 21727-21739.

Drew, A.R., Snay, R.A. (1989), DYNAP: software for estimating crustal deformation from geodetic data. Tectonophysics, 162, 331-343.

Dzurisin, D. (2006), Volcano Deformation : New Geodetic Monitoring Techniques. Springer-Verlag, New York.

El-Fiky, G., Kato, T., Oware, E.N. (1999), Crustal deformation and interpolate coupling in the Shikoku district, Japan, as seen from continuous GPS observation. Tectonophysics. 314, 387-399.

Eren, K. (1984), Strain Analysis Along the North Anatolian Fault By Using Geodetic Survey. Bulletin Géodésique. 58 (2.), 137-150.

Fernández-Ros, A. (2006), Modelización de movimientos y deformaciones de la corteza terrestre mediante observaciones de los satélites GPS (Aplicación al volcán Decepción). Ph. Tesis. Universidad de Cádiz.

Garcia, A.; Blanco, I.; J.M. Torta; M.M. Astiz; J.M. Ibáñez And R. Ortiz (1997), A search for the volcanomagnetic signal at Deception volcano (South Shetland I., Antarctica) Ann. Geofis. 40 (2): 319-327.

González-Ferrán O (1991), The Bransfield rift and its active volcanism. Thomson R. A, Crame J. A, Thomson J. W (eds.) Geological Evolution of Antarctica. Cambridge University Press, Cambridge, 505-509.

Grafarend, E. And Voosoghi, B. (2003), Intrinsic deformation analysis of Earth's surface based on displacement fields derived from space geodetic measurements. Case studies: present-day deformation patterns of Europe and the Mediterranean area (ITRF data sets). Journal of Geodesy. 77 (5-6) pp 303-326.

Ibáñez J, Del Pezzo E, Almendros J, La Rocca M, Alguacil G, Ortiz R, García A (2000), Seismovolcanic signals at Deception Island Volcano, Antarctica: Wavefield analysis and source modelling. J Geophys Res 105: 13905-13931.

Mantovani, E., Cenni, N., Alberello, D., Viti, M., Babbucci, D., Tamburelli, C. , D'onza, F. (2001), Numerical simulation of the observed strain field in the central-eastern Mediterranean region. Journal of Geodynamics, 31, 519-556.

Murray, J.B., Wooller, L.K. (2002), Persistent summit subsidence at Volcán de Colima, Mexico, 1982-1999: strong evidence against Mogi deflation. Journal of Volcanology and Geothermal Research. 117 (1-2), 69-78.

Vanícek, P., Krakiwsky, E. (1986), Geodesy: The Concepts (Second Edition). Elsevier Science. Ámsterdam, The Netherlands. 1986.

Vila, J., Ortiz, R., Correig, A.M. Y Garcia, A. (1992), Seismic activity on Deception Island. Yoshida, Y., Kaminuma, K. y Shiraishi, K. (Eds.), Recent Progress in Antarctic Earth Science, 449-456, Tokyo, Terra Scientific Publishing Company

Ward, S.N. (1998), On the consistency of earthquake moment rates, geological fault data, and space geodetic strain: the United States. Geophysical Journal International. 134 (1) pp. 172-186.